

Orientation Development in Retensitized, Biaxially Oriented Polypropylene Films

JOAN M. STROBEL* and SEHYUN NAM

3M Company, 3M Center, Building 230-1E-04, St. Paul, Minnesota 55144

SYNOPSIS

A basic study of orientation development in retensitized, biaxially oriented polypropylene films was performed. Wide-angle X-ray scattering (WAXS) and birefringence measurement techniques were used to examine films prepared under specific processing conditions. Biaxial orientation factors were determined for these films and were correlated with end-use properties of the materials. In particular, the dispensability of oriented polypropylene films was found to correlate with crystalline-phase and amorphous-phase orientation factors. Dispensability is a relatively important property of pressure-sensitive tapes; it is defined as the force necessary to cut a film backing over a serrated blade of the type used in commercially available adhesive-tape dispensers.

INTRODUCTION

Oriented polypropylene (OPP) films exhibit excellent cost versus performance characteristics. The use of polypropylene films produced via *biaxial* orientation processes has accounted for most of the growth in polypropylene film consumption in the early 1980s.¹ BOPP films are in widespread commercial use in a number of applications, including pressure-sensitive-adhesive tape constructions.

Because of the commercial importance of oriented-polypropylene films, many investigators²⁻⁹ have studied the interactions between processing conditions, polymer structure, and end-use properties for these materials. The amount of fundamental structural information available for both uniaxially oriented and biaxially oriented films has expanded through use of techniques such as wide-angle X-ray scattering, birefringence measurements, sonic-modulus determinations, and infrared dichroism measurements. Through application of these techniques, a general understanding has emerged of the importance of the various structural parameters used to characterize the state of orientation in films and the extent that various end-use properties are de-

termined by these parameters. For example, Samuels²⁻⁴ found that, for uniaxially oriented polypropylene films, many properties correlate well with the corresponding variations in molecular orientation of the amorphous phase. Samuels also provided considerable evidence for the existence of general structure-versus-property correlations which are independent of the fabrication scheme. Nadella et al.⁵ found strong correlations between various physical properties and the total birefringence of oriented polypropylene fibers. DeVries⁶⁻⁸ has shown that many properties of biaxially oriented polypropylene films are dependent on average orientation.

The purpose of our paper is to present the results of a basic study of the development of structure in retensitized, biaxially oriented polypropylene films. Retensitized film is produced by restretching the film in the longitudinal direction *following* biaxial orientation. We seek to relate the structural characteristics of the films to end-use properties, particularly to film dispensability. Dispensability is a relatively important property of pressure-sensitive tapes; it is defined as the force (N) necessary to cut a film backing over a serrated blade of the type used in commercially available adhesive-tape dispensers.

EXPERIMENTAL

A polypropylene resin from Fina Oil and Chemical Co. with a melt index¹⁰ of 1.1 was used in this study.

* To whom correspondence should be addressed.

This material had a polydispersity index of 5.7 as determined using high-temperature size exclusion chromatography.¹¹ The resin contained small amounts of antioxidant and acid scavenger.

Biaxially oriented films were produced using this polypropylene resin on a tenter-frame film line equipped with a retensitizer.¹² A series of six films was produced, as described in Table I. The initial thickness of the extruded sheet was kept constant so that quenching conditions for all samples would be equivalent. Therefore, final film thicknesses after drawing were not constant, but decreased as the machine-direction (MD) draw ratio was increased. The casting wheel was maintained at about 40°C; the speed of the casting wheel was adjusted to produce a 2.16 mm extruded sheet. The extruded sheet was then passed over a series of heating rolls with surface temperatures of 125°C. The heated sheet was stretched between two nipped drawing-rolls rotating at different speeds to attain a first draw ratio of 5 : 1 in the MD. The transverse-direction (TD) draw ratio was 6 : 1 for all samples. This draw ratio was achieved by feeding the longitudinally oriented sheet into a tenter oven with multiple heating zones. The oven set-point temperatures in the heating zones ranged from 162 to 168°C.

The tentered film was then stretched between two nipped retensilizing-rolls that were maintained internally at 163°C. These drawing rolls were rotated at different speeds to longitudinally draw the film for a second time at overall draw ratios ranging from 1.4 : 1 to 2.3 : 1. The strain rates of retensilizing in the two draw gaps were of the order of 30,000 and 13,000%/min, respectively.

The films were analyzed using a combination of differential scanning calorimetry, birefringence, and wide-angle X-ray scattering (WAXS) measure-

ments. In addition, physical properties and dispending forces were determined for all samples.

Differential scanning calorimetry was performed on a DuPont 912 dual cell differential scanning calorimeter at a scan rate of 10°C/min. Heats of fusion were measured for all samples and percent crystallinities were determined assuming a value of 201 J/g as the heat of fusion for 100% crystalline polypropylene.¹³

Birefringence values were measured using a rotary Eringhaus calcite compensator in the plane of the film and as a function of the angle of inclination of the film with respect to the incident light beam, following the procedure described by Stein.¹⁴

Wide-angle X-ray scattering was used to determine the intensity distribution function needed for pole-figure plotting and determination of the $\cos^2 \phi$ functions used to compute the crystalline orientation factors. These results were obtained applying the techniques developed by Heffelfinger and Burton.¹⁵ For each sample, sheets of film were stacked with the machine-directions aligned. The sheets were glued together along the edges and mounted on a single-crystal orienter. The single-crystal orienter was then mounted on a General Electric XRD-5 Diffractometer. CuK_α radiation with a wavelength of 1.542 Å was used. The diffractometer was set at a fixed diffraction angle, 2θ , for diffraction from either the (110) or (040) planes. Each sample was rotated and tilted by the single-crystal orienter in order to determine the intensity distribution function.

Crystalline orientation factors were determined using the following equations, as defined by White and Spruiell¹⁶:

$$f_{1j}^B = 2 \cos^2 \phi_{j1} + \cos^2 \phi_{j2} - 1 \quad (1)$$

$$f_{2j}^B = 2 \cos^2 \phi_{j2} + \cos^2 \phi_{j1} - 1. \quad (2)$$

In these equations, j represents a crystallographic axis and $\cos^2 \phi_{jk}$ is the average value of the square of the cosine of the angle between the j crystallographic axis and the reference direction, k ($k = 1$ for the machine direction and $k = 2$ for the transverse direction).

The b -axis crystalline orientation factors were computed using the above equations and the (040) intensity distribution, since the (040) planes are perpendicular to the b -axis in monoclinic polypropylene. The c -axis, which is parallel to the helical axis of the polypropylene chain, does not have a perpendicular set of reflecting planes. Therefore, equations derived by Wilchinsky,¹⁷ which relate the variation in the intensity distribution in the (110)

Table I Summary of Retensitized, Biaxially Oriented Polypropylene Films Prepared

Film Designation	MD Draw Ratio ^a	Thickness (mm) ^b
R1	7.25 : 1	0.046
R2	8.25 : 1	0.041
R3	9.60 : 1	0.036
R4	10.5 : 1	0.032
R5	11.0 : 1	0.030
R6	11.5 : 1	0.030

^a The transverse-direction (TD) draw ratio was 6.0 : 1 for all samples.

^b The reported thicknesses are average values using ten measurements for each sample. The standard deviation for each thickness is ± 0.001 mm.

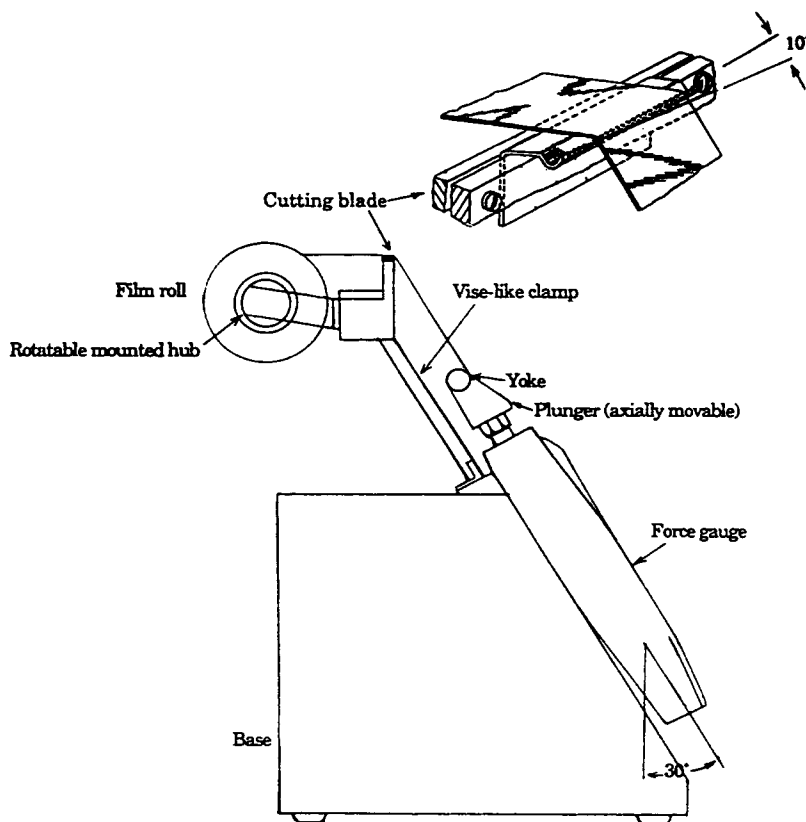


Figure 1 Schematic diagram of dispensing-force test apparatus.

and (040) reflections to the $\cos^2\phi_{ck}$ values, were used in computation of the c -axis orientation factors. Orientation factors were also determined for an a' -axis, which is perpendicular to the plane of the b and c axes. The true a axis is not perpendicular to the plane of the b and c axes, but differs by 9.2° because of the monoclinic structure of the polypropylene unit cell.

Physical properties were measured for all films using a dual-speed Instron Tensile Tester in accordance with Method A of ASTM D882-83.¹⁸ The grips of the apparatus were initially spaced at 10.16 cm for each test. An initial crosshead speed of 5.08 cm/min was used for the first 6% of sample elongation. A crosshead speed of 25.4 cm/min was used for the remainder of each test.

Dispensing forces were measured using the test device and procedure described by Wong et al.¹² Dispensing force is the force necessary to cut or dispense a film over a cutting blade of the type used in commercially available adhesive-tape dispensers. The device for measuring dispensing force is illustrated in Figure 1. The device consists of a base supporting a viselike clamp; the clamp is adapted to fix the cutting blade at an angle of about 10° to the

horizontal. The clamp also holds a projecting bracket on which a rotatable hub is attached; the hub supports the roll of film to be tested. A force gauge for recording the force required to sever the film includes an axially movable plunger which has a yoke on one end to support the film. The end of the plunger opposite the yoke is mounted so that it can slide axially (the sliding mechanism is not shown in the figure) and is coupled to a mechanism that records the maximum outward force applied to the plunger. The gauge can be moved from an initial test position to a final test position at a constant speed of 0.76 m/min. The path of movement of the plunger is at an angle of about 30° with respect to the vertical.

RESULTS

The crystallinities of the various polypropylene films produced for this study are listed in Table II. The levels of crystallinity are of the order of 60% for all samples.

Birefringence results for the polypropylene films are summarized in Table II and are plotted as a function of machine-direction draw ratio in Figure

Table II Birefringence and Percent Crystallinity for Retensitized Oriented Films^a

Sample	Birefringence $\times 10^3$			% Cryst
	Δn_{12}	Δn_{13}	Δn_{23}	
R1	10.5	18.1	7.5	62
R2	13.1	22.1	9.0	63
R3	16.2	21.7	5.6	61
R4	18.6	23.6	5.0	56
R5	19.9	24.5	4.6	65
R6	20.1	24.4	4.3	61

^a The subscripts 1, 2, and 3 refer to the machine, transverse, and thickness directions of the film, respectively. Δn is the difference in refractive index between the specified film directions. The standard deviation for Δn_{12} is $\pm 0.5 \times 10^{-3}$. The standard deviation for Δn_{13} is $\pm 10 \times 10^{-3}$. The standard deviation for percent crystallinity is $\pm 5\%$.

2. Birefringence in polypropylene films is primarily related to the orientation of polymer chains. As seen in Figure 2, Δn_{13} and Δn_{12} are positive and increase with increasing draw ratio; Δn_{23} is positive and decreases slightly with increasing draw ratio. These results are in general agreement with those presented by Shimomura, Spruiell, and White⁹ for polypropylene tubular films produced at constant blowup and increasing drawdown ratios. DeVries⁶ reported negative and increasing values of Δn_{12} and positive and increasing values of Δn_{13} for biaxially oriented polypropylene films of increasing machine-direction draw ratio. Δn_{23} was positive and decreased slightly as machine-direction draw ratio increased. These biaxially oriented films were also produced

on a tenter frame film line; however, drawing in the cross direction was the final orientation step.

For an orthorhombic crystalline phase, White and Spruiell¹⁶ have shown that the birefringences Δn_{13} and Δn_{23} are related to the biaxial orientation factors through the relations

$$\Delta n_{13} = X(\Delta_{ca}^{0c} f_{1c}^B + \Delta_{ba}^{0c} f_{1b}^B) + (1 - X)\Delta^{0a} f_1^B + (\Delta n_{13})_{\text{form}} \quad (3)$$

$$\Delta n_{23} = X(\Delta_{ca}^{0c} f_{2c}^B + \Delta_{ba}^{0c} f_{2b}^B) + (1 - X)\Delta^{0a} f_2^B + (\Delta n_{23})_{\text{form}} \quad (4)$$

The variables in these expressions are defined as follows: Δn_{13} and Δn_{23} are film birefringences, where the subscripts 1, 2, and 3 refer to the machine, transverse, and thickness directions of the films, respectively. X is the crystalline-phase weight fraction. $(1 - X)$ is the amorphous-phase weight fraction. $\Delta_{ca}^{0c} = n_c - n_a$ and $\Delta_{ba}^{0c} = n_b - n_a$, where n_c , n_b , and n_a are the refractive indices along the c , b , and a crystallographic axes of a polypropylene single crystal, respectively. Δ_{ca}^{0c} and Δ_{ba}^{0c} are intrinsic birefringences of the crystalline phase. f_{1c}^B , f_{1b}^B , f_{2c}^B , and f_{2b}^B are crystalline orientation factors, as defined by eqs. (1) and (2). Δ^{0a} is the intrinsic birefringence of the amorphous phase. f_1^B and f_2^B are orientation factors for the amorphous regions. $(\Delta n_{13})_{\text{form}}$ and $(\Delta n_{23})_{\text{form}}$ are form birefringences due to the phase distribution.

Thus, assuming (1) a two-phase model of polypropylene, (2) an orthorhombic crystalline phase, (3) form birefringences ≈ 0 , and (4) $n_a \approx n_b$, amorphous orientation factors can be determined using

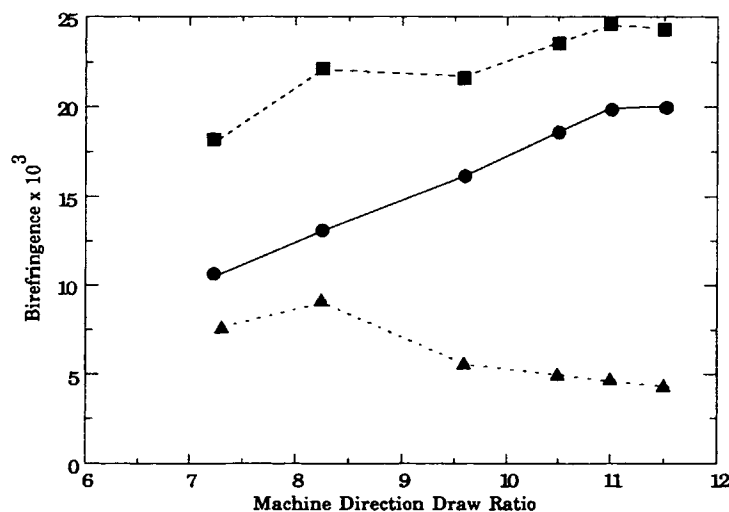
**Figure 2** Variation of birefringence with draw ratio: (■) Δn_{13} ; (●) Δn_{12} ; (▲) Δn_{23} .

Table III Orientation Factors for Polypropylene Films

Sample	Crystalline Orientation Factors						Amorphous Orientation Factors	
	c-axis		b-axis		a'-axis		f_1^B	f_2^B
	f_{1c}^B	f_{2c}^B	f_{1b}^B	f_{2b}^B	$f_{1a'}^B$	$f_{2a'}^B$		
R1	0.464	0.228	-0.405	-0.335	-0.059	0.106	0.434	0.155
R2	0.474	0.192	-0.419	-0.339	-0.055	0.147	0.610	0.250
R3	0.443	0.073	-0.355	-0.273	-0.089	0.200	0.598	0.183
R4	0.469	0.052	-0.345	-0.256	-0.124	0.204	0.611	0.156
R5	0.569	0.100	-0.415	-0.305	-0.154	0.206	0.672	0.132
R6	0.458	0.065	-0.355	-0.266	-0.103	0.201	0.703	0.136

birefringence data and crystalline-phase orientation factors determined from WAXS measurements.

Crystalline orientation factors were determined from the intensity distribution data, as described previously. Amorphous orientation factors were cal-

culated using values of $n_c = 1.5407$, $n_a \approx n_b = 1.5124$, and $\Delta^{0a} = 0.060$.¹⁹ These results appear in Table III.

Figure 3 shows a graphical representation of the state of orientation in the film samples obtained by plotting the orientation factor data from Table III

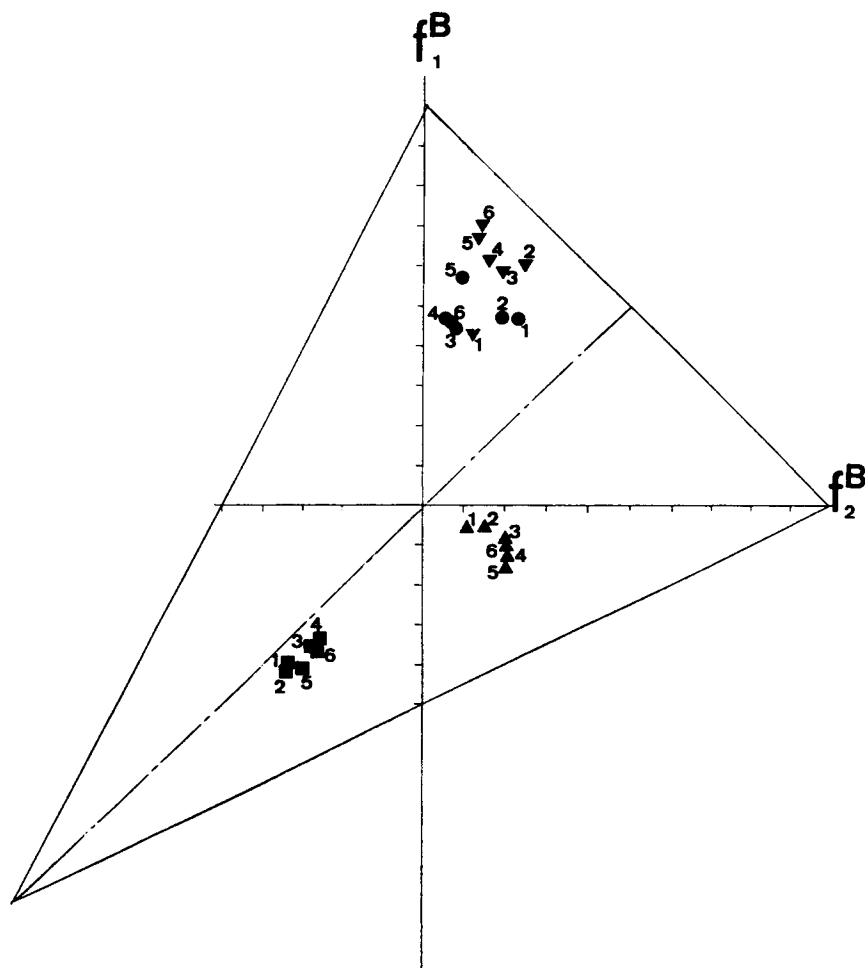


Figure 3 Orientation triangle diagram for polypropylene films: (●) c-axis; (■) b-axis; (▲) a'-axis; (▼) amorphous.

on an orientation triangle diagram.¹⁶ All states of orientation, as described by the biaxial orientation factors, are considered to lie within an isosceles triangle. Isotropic systems are located at the origin. States of uniaxial orientation with respect to the machine and transverse directions lie along the respective coordinate axes. The three apices of the triangle represent states of perfect uniaxial orientation. Equal planar orientation is represented by the point $(\frac{1}{2}, \frac{1}{2})$ and all points along the base of the triangle represent orientations within the plane of the film.

For the samples shown in Figure 3, there is a trend towards increasing alignment of the amorphous phase along the machine direction as a function of increasing machine-direction draw ratio. The crystalline-phase orientation factors show no definite trends, although there does appear to be a decrease in the biaxial nature of the films with increasing machine-direction draw ratio.

According to DeVries,⁶ the fraction of axial orientation with respect to the machine direction φ_{ax}^{MD} , observed in biaxially oriented polypropylene films, can be expressed by the following proportionalities for the crystalline and amorphous phases, respectively:

$$\varphi_{ax,c}^{MD} \propto (f_{1c}^B - f_{2c}^B)_c \quad (5)$$

$$\varphi_{ax,am}^{MD} \propto (f_1^B - f_2^B)_{am} \quad (6)$$

Table IV summarizes the fractions of axial orientation for the polypropylene film samples of this study. For both the crystalline and amorphous phases, the degree of axial orientation increases as machine-direction draw ratio increases. This result is consistent with the results presented by DeVries⁶ for uniaxially drawn films and for highly unbalanced biaxially drawn films.

The (040) and (110) pole distributions for samples R1, R3, and R5 are shown in Figure 4. The (040) pole figures, which represent the orientation

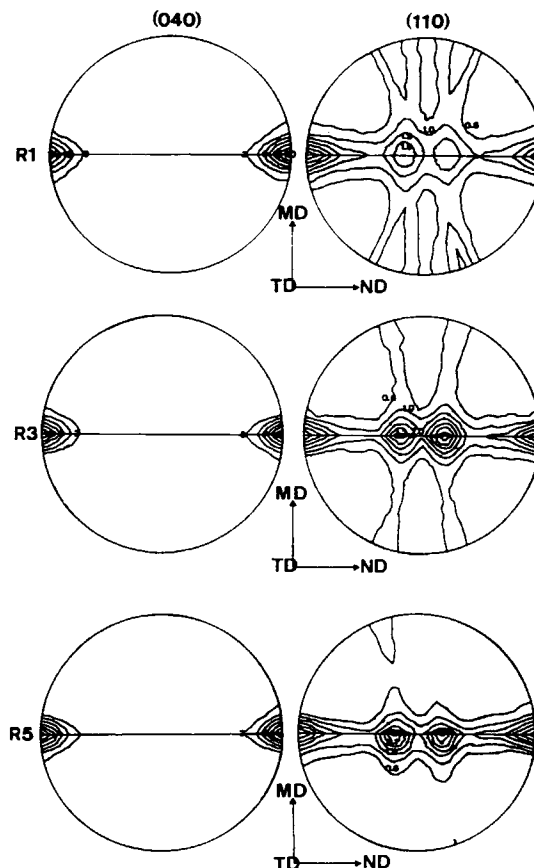


Figure 4 Pole figures for the (040) and (110) planes for film samples R1, R3, and R5.

of the *b* crystallographic axis, exhibit the most distinctive features. The (040) poles are very concentrated in the normal direction for all samples. The (110) pole figures are quite complicated. The (110) poles concentrate approximately perpendicular to the machine direction and are distributed fairly uniformly about it. There is also a tendency for the (110) poles to concentrate near the transverse direction.

Average physical property values and average dispensing forces for the polypropylene film samples appear in Table V. Ten samples, five normal and five parallel with the principal axis of anisotropy of the film, were tested for each value reported. Each dispensing force value is the average of ten individual measurements. At the test conditions used for property measurements, the machine-direction moduli and break strengths increase as machine-direction draw ratio increases. Machine-direction elongation at break decreases as machine-direction draw ratio increases. The dispensing force per unit sample thickness also decreases as machine-direction draw ratio increases. Both sharp-blade dispensing force

Table IV Axial Orientation in Polypropylene Films

Sample	$\varphi_{ax,c}^{MD}$	$\varphi_{ax,am}^{MD}$
R1	0.236	0.279
R2	0.282	0.360
R3	0.370	0.415
R4	0.417	0.455
R5	0.469	0.540
R6	0.393	0.567

Table V Physical Properties and Dispensing Forces for Polypropylene Films

Sample	Secant Modulus at 1% Elongation (GPa)		MD Break Strength (GPa)	MD Elongation at Break (%)	Dispensing Force (N/mm × 10 ⁻²)	
	MD	TD			Sharp ^a Blade	Dull Blade
R1	2.7	2.1	0.29	67	3.7	15
R2	2.8	2.1	0.33	55	3.5	13
R3	3.5	2.1	0.37	46	3.0	12
R4	3.9	2.1	0.39	34	3.0	12
R5	4.1	2.1	0.42	33	2.5	11
R6	4.3	2.1	0.42	31	2.8	10

^a Sharp blade refers to a new dispensing blade, as provided on commercially available adhesive-tape dispensers. Dull blade refers to a dispensing blade which has been dulled by mechanical abrasion to simulate dulling through normal use or damage. In general, dull blade dispensing results allow more discrimination between the various samples. The standard deviations for the various properties are as follows: MD and TD secant moduli, ±0.05 GPa; MD break strength, ±0.007 GPa, MD elongation at break, ±2%; sharp-blade dispensing force, ±0.3 × 10⁻² N/mm; dull-blade dispensing force, ±1 × 10⁻² N/mm.

and dull-blade dispensing force are dependent upon sample thickness. There is no simple correlation between dispensing force and thickness; however, a linear relationship was assumed for this study. This assumption is reasonable since the range of specimen thickness is not large.

Figures 5–9 show the relationships between the properties from Table V and the degree of axial orientation. The lines drawn in the figures represent the best fit of the data using simple linear regression; the quality of the fit varies considerably. As the degree of axial orientation increases in both the crys-

talline and amorphous phases, modulus and break strength increase and break elongation and dispensing force decrease.

Samuels⁴ found that, for uniaxially oriented polypropylene films tested at *low* rates of deformation, the true fracture stress (rupture force/cross-sectional area of the sample at break) is independent of the initial state of orientation of the sample, as described by an average orientation factor. At *high* rates of extension, the true fracture stress was found to be a direct function of the initial state of orientation of the sample. Similar results were obtained

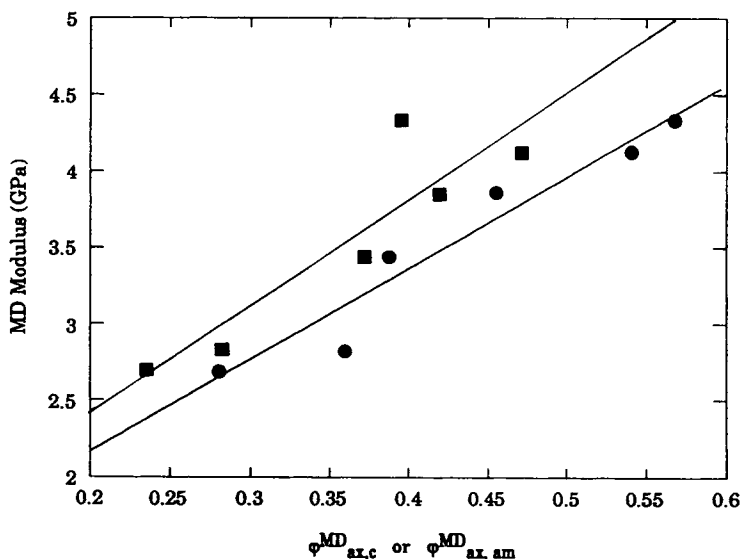


Figure 5 Relation between the degree of axial orientation, $\varphi_{ax,c}^{MD}$ (■) or $\varphi_{ax,am}^{MD}$ (●), and modulus for polypropylene film samples.

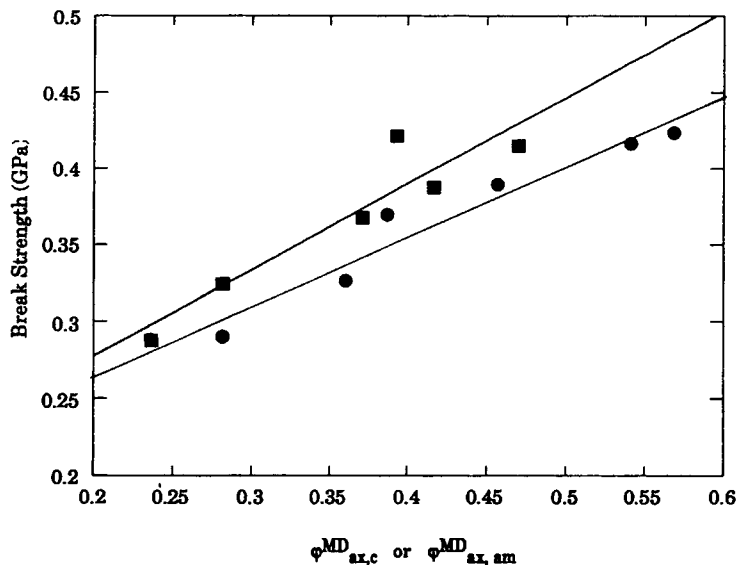


Figure 6 Relation between the degree of axial orientation, $\varphi_{ax,c}^{MD}$ (■) or $\varphi_{ax,am}^{MD}$ (●), and break strength for polypropylene film samples.

for the fracture strain. DeVries⁷ confirmed these results for uniaxially drawn films, but found that the true fracture stress is not dependent upon degree of orientation for *biaxially* oriented films. This is because an increase in sample tenacity (rupture force/initial cross-sectional area of the sample) is compensated for by a decrease in rupture strain with increasing degree of orientation. DeVries found that tenacity *is* a rapidly increasing function of initial degree of orientation and correlates well with bire-

fringence in both uniaxially and biaxially drawn films. As seen in Figure 6, break strength, or tenacity, does appear to correlate well with both crystalline-phase and amorphous-phase axial orientation factors for the samples prepared in this study.

Sharp-blade and dull-blade dispensing forces are plotted in Figures 8 and 9 as functions of the crystalline-phase and amorphous-phase axial orientation factors. Both dispensing forces appear to decrease as axial orientation in both phases increases.

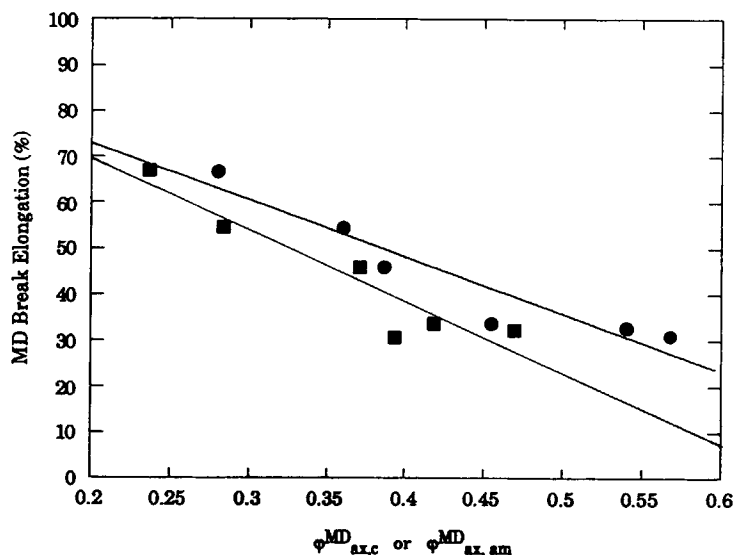


Figure 7 Relation between the degree of axial orientation, $\varphi_{ax,c}^{MD}$ (■) or $\varphi_{ax,am}^{MD}$ (●), and break elongation for polypropylene film samples.

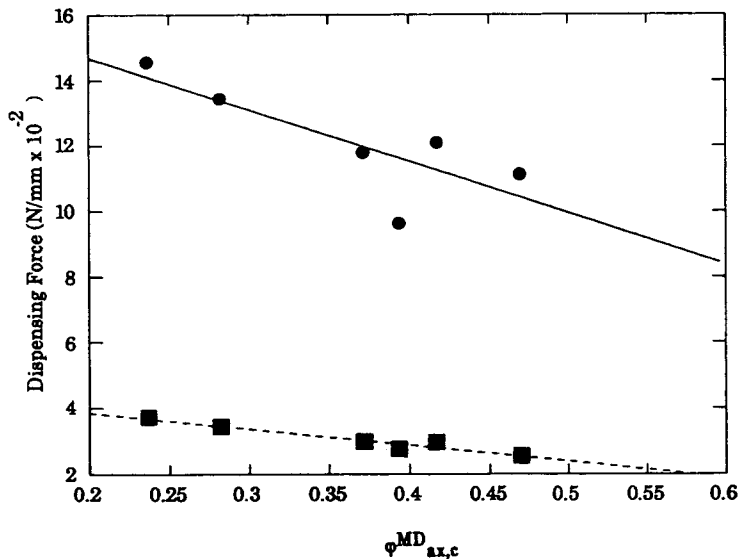


Figure 8 Relation between the degree of crystalline axial orientation, $\varphi_{ax,c}^{MD}$, and sharp blade dispending force (■) or dull blade dispending force (●).

DeVries⁷ reported initial tear resistance results for biaxially oriented polypropylene films using the tensile test described in ASTM D1004. Although this test is not completely analogous to the dispending test used in the present study, there are similarities in the results obtained. DeVries⁷ found that failure in biaxially drawn films was ductile and that, for nearly balanced films, was practically identical in both the MD and TD directions and equal to about 4 N. The sharp blade dispending force for the most

nearly balanced film produced in our study was 3.7 N. DeVries also reported a decrease in the initial tear resistance of his samples with increasing average orientation with respect to the direction of tear propagation. He concluded that tear initiation in unbalanced biaxially oriented films is approximately the same in all directions except the direction of maximum molecular orientation; this direction is associated with lower initial tear resistance values. The direction of maximum molecular orientation is

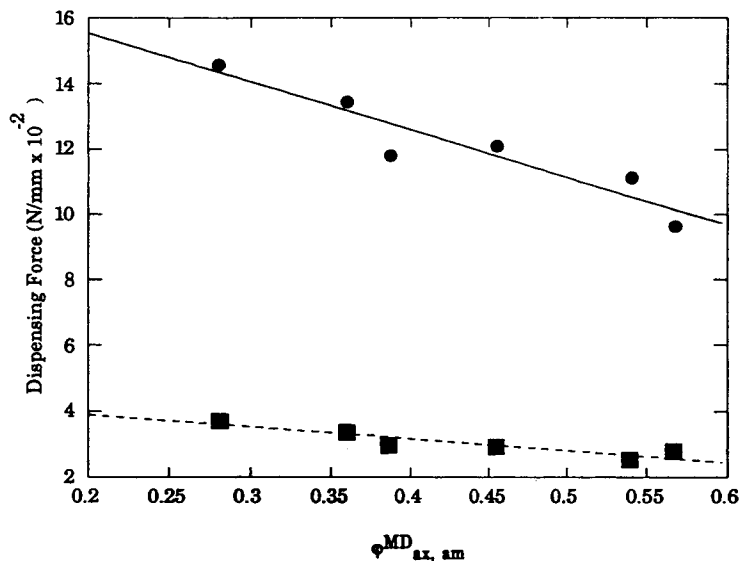


Figure 9 Relation between the degree of amorphous axial orientation, $\varphi_{ax,am}^{MD}$, and sharp blade dispending force (■) or dull blade dispending force (●).

also associated with lower dispensing force values in our study.

DISCUSSION

Dispensing can be thought of as a two-step process that occurs at each tip along a serrated dispenser blade: puncture initiation and tear propagation. The ease of dispensing a film is determined to a large extent by film resistance to puncture initiation. Under proper deformation conditions, such as those applied in commercially available adhesive-tape dispensers, puncture formation will occur in oriented polypropylene film backings. Opposed to this failure mechanism is the ability of the film to plastically deform to relieve the applied stress.

As shown in Figure 5, the film backings become stiffer as the degree of orientation increases. Hence, the more highly oriented films are more resistant to plastic deformation (see Fig. 7). As the crystallites and the molecules in the amorphous phase become more highly oriented, the samples respond as though they were being pulled at even faster rates of deformation.⁴ At sufficiently high rates of deformation, the molecules do not have much mobility. These films exhibit low extension and dispense more easily.

The observed mechanical properties of the films are a consequence of the internal structure of the samples at the time of testing. Since polypropylene is comprised of a crystalline phase and an amorphous phase, the properties exhibited by the samples are due to the response of either one or both of the phases. As shown in Figures 8 and 9, both sharp and dull blade dispensing forces decrease as axial orientation in the crystalline and amorphous phases increases. Therefore, it seems reasonable that the dispensing results obtained in this study are dependent upon the state of orientation in both the crystalline and amorphous phases.

CONCLUSIONS

In our work, we have shown that the degree of molecular orientation achieved in the production of re- tensilized biaxially oriented polypropylene films is a significant determinant of the physical properties of the films. Orientation in both the crystalline and

amorphous phases has been shown to contribute to the observed properties and in particular to dispensability characteristics. Our data suggest that further improvements in dispensing characteristics might be achieved through additional increases in amorphous orientation. These conclusions demonstrate the importance of using structural parameters to describe processing/end-use performance interactions in oriented films.

We would like to thank Dr. Joseph E. Spruiell of the University of Tennessee for his assistance in obtaining the wide-angle X-ray scattering results.

REFERENCES

1. R. B. Lieberman and P. C. Barbe, in *Encyclopedia of Polymer Science and Engineering*, Wiley, New York, 1988, Vol. 13, p. 517.
2. R. J. Samuels, *Structured Polymer Properties*, Wiley, New York, 1974, Chap. 4.
3. R. J. Samuels, *Polym. Eng. Sci.*, **16**, 327 (1976).
4. R. J. Samuels, *Polym. Eng. Sci.*, **19**, 68 (1979).
5. H. P. Nadella, J. E. Spruiell, and J. L. White, *J. Appl. Polym. Sci.*, **22**, 3121 (1978).
6. A. J. DeVries, *Pure Appl. Chem.*, **53**, 1011 (1981).
7. A. J. DeVries, *Pure Appl. Chem.*, **54**, 647 (1982).
8. A. J. DeVries, *Polym. Eng. Sci.*, **23**, 241 (1983).
9. Y. Shimomura, J. E. Spruiell, and J. L. White, *J. Appl. Polym. Sci.*, **27**, 2663 (1982).
10. ASTM D1238-86, Condition L, ASTM Standards (1987).
11. V. Grinshpun and A. Rudin, *J. Appl. Polym. Sci.*, **30**, 2413 (1985).
12. R. Wong, J. J. Pedginski, and A. H. Wong, U.S. Pat. 4,451,533 (1984).
13. J. R. Knox, in *Analytical Calorimetry*, R. S. Porter and J. F. Johnson, Eds., Plenum, New York, 1968, p. 14.
14. R. S. Stein, *J. Polym. Sci.*, **24**, 383 (1957).
15. C. J. Heffelfinger and R. L. Burton, *J. Polym. Sci.*, **47**, 289 (1960).
16. J. L. White and J. E. Spruiell, *Polym. Eng. Sci.*, **21**, 859 (1981).
17. Z. W. Wilchinsky, *J. Appl. Phys.*, **31**, 1969 (1960).
18. ASTM D882-83, Method A, ASTM Standards (1983).
19. J. C. Seferis and R. J. Samuels, *Polym. Eng. Sci.*, **19**, 975 (1979).

Accepted February 26, 1990